Design and Manufacturing of Heading Machine Prototype

Boris Fedorov, Harald T. Rieber, Henry Ly, Rishabh Roy
University of California, Berkeley
2521 Hearst Ave, Berkeley, California, USA

Abstract
This paper elucidates the design and manufacturing process of a prototype billet heading machine that uses plasticine at room-temperature as a substitute for steel at high temperature. In particular, the mechanical design, material selection, and learnings from the prototype are discussed. Continuous billet feeding could have major cost implications for engineers during the manufacturing process because hot-worked steel heading, which is a cost-intensive process, can potentially be modeled in the real world with a much cheaper down-scaled prototyping machine. Continuous billet feeding also allows the heading machine to be semi-automated, leading to higher production volumes and significant labor cost savings. It was shown that although our prototype is scaled down, high stiffness materials were still required for some components in order to minimize deflection. Additionally, it is critical to minimize deflection without over constraining components for the machine to produce bolts within specification.

Introduction
Heading operations are a manufacturing method of choice for producing fasteners in many industries. Heading works by applying a punching-force to a material contained in a die, thus causing plastic deformation to form a desired part [1]. The primary benefits of using heading instead of a subtractive manufacturing method are the material cost savings from creating little to no waste material, and the improved grain structure of the final product, as the grains in the bolt-head will better align with the grains in the shaft as seen in Fig. 1 [1]. However, heading machines represent a significant capital investment, which is why it is mostly used for medium to high volume manufacturing. In industry, it is common for stock material to be cut to size, heated in an induction coil, and then loaded manually into the heading machine by an operator. For our project, we specifically looked at Sutherland's HCP-330-FLST heading machine to aid in our design and process specification as our real-life machine model [2]. The design and material selections were largely driven by theoretical stress calculations and beam bending equations that were later validated with simulations [3].

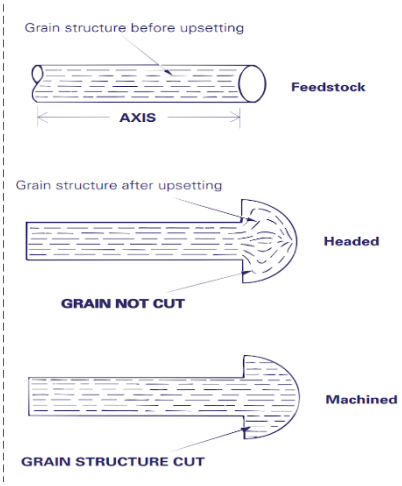

Fig. 1 – Improved grain structure due to heading vs. subtractive manufacturing

The primary success criterion of the project was to design and build a prototype of a heading machine that could successfully produce a finished bolt. However, secondary goals based on automation, speed of the machine, and the dimensional accuracy of the finished product were also considered as necessary metrics for prototype validation.

Experimental
Design
As seen in Fig. 2 and Fig. 3, the preliminary designs of our prototype had a configuration where the billet would be fed into the machine, cut to length and an intermediary piece would be inserted between the cut

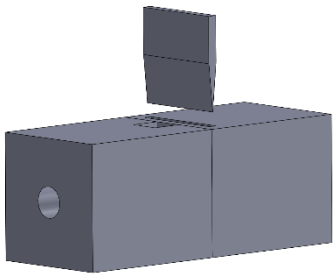

Fig. 2 – Initial Design

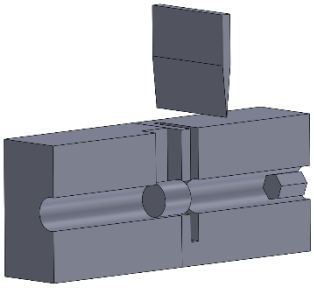

Fig. 3 – Initial Design Cross Section

billet section and the remaining billet to serve as an ejector pin. Then the die would punch into the cut billet, forming the head, and the finished part and ejector pin would be pushed out by the remaining billet before the next cycle. This preliminary concept was a useful evolutionary step towards the final design where there is no need for an ejector pin.

The final design of our prototype shown in Fig. 4 consists of three main compartments. The first compartment shown in Fig. 5 is the billet housing compartment where the billet is loaded by a conveyor belt system powered by two motors. In the second compartment, shown in Fig. 6, the billet is cut into its appropriate length for heading by a blade actuated by two DC motors. The third compartment shown in Fig. 7 is where the heading process occurs. A linear actuator is used to actuate the upper die for the heading process. The three major compartments are held in place with an acrylic frame on the sides and top and A36 Steel at the bottom to counteract the forces and moments generated by the linear actuator.

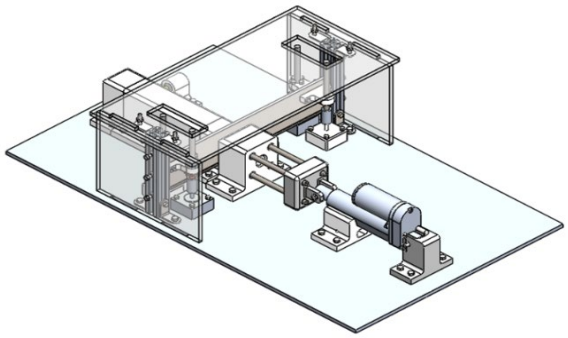

Fig. 4 – Final Prototype Design

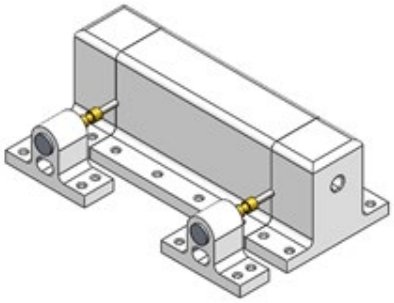

Fig. 5 – Billet Housing Compartment

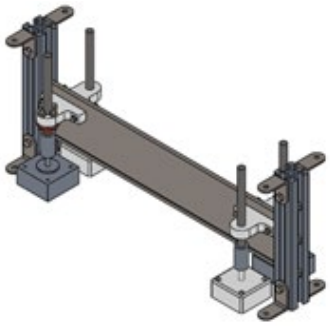

Fig. 6 – Cutting Compartment

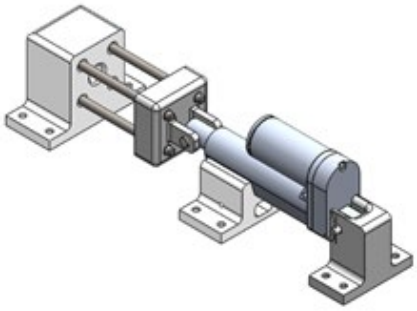

Fig. 7 – Heading Compartment

Using the calibration curve of linear actuator load (lbs.) versus current (amps), applied load can be determined by measuring the linear actuator's current draw during the heading operation. This will allow us to validate the theoretical heading force we derived from our calculations. As seen in Fig. 8, we will use the red line for a M10 bolt and the green line for a M20 bolt [4]. A M10 Bolt requires a theoretical Heading Force of 33.65 lbs. and a M20 Bolt requires a theoretical Heading Force of 67.31 lbs. The hand calculation used to derive our theoretical Heading Force is shown in Appendix B.

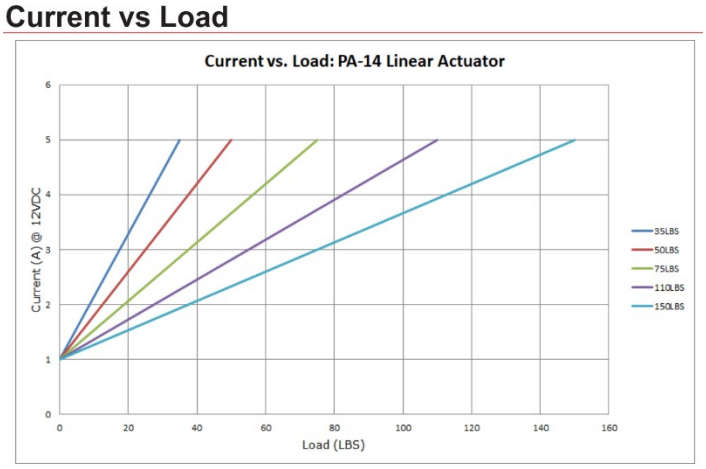

Fig. 8 – Linear Actuator Calibration Curve

Testing and Evaluation

We plan to test our machine using Fishbone or Ishikawa Diagrams [5]. For our DFM project we will analyze the following 5 Ms: Man, Machine, Material, Method and Measurement. The specifics of our testing plan are shown in Table 1 below.

We will also determine the success of our heading machine based on three criteria. The first criterion is the bolts per minute rate, which will determine if the machine has a comparable speed to the examined real-life machine. The target is to produce five bolts per minute which would make the design faster than current industry methods and achieve the goal of increasing production volumes. The second criterion is the level of automation, ideally the only action a human operator will need to assist with is the loading of the stock material; if this is achieved

our design could bring down labor costs. Finally, the third success criterion is a dimensional specification to have all dimensions of the final bolt within a ±0.25mm tolerance.

Table 1 – Testing table using Ishikawa Diagram elucidating the 5 M's: Man, Machine, Material, Method, and Measure

	Test Name	Test Description	Specification
MAN	Bolt Unloading (dimensional)	Test that the bolt can be removed without changing the dimensions of the finished bolt	Dimensional tolerance: ±0.1"
MACHINE	Heading Force	Test that the applied load meets our specifications	50 lbs.
	Heading Alignment	Test that the two parts of the die line up correctly when pressing down	Dimensional tolerance: ±0.1" Concentricity: ±0.01"
	Overall Machine Stiffness	Test that the machine is sufficiently stiff	No visible deflection through whole process, ±2.5mm deflection
MATERIAL	Blank Testing	Ensure that the blank/billet meets the design specifications	Dimensional tolerance: ±0.1" Volumetric tolerance: ±0.5 in^3
	Material Waste	Ensure that minimal material is wasted in the process; minimal flash	Minimal flash discharge: ±0.5 in^3
METHOD	Material Feeding	Material is fed the correct length. Frictional heating of the machine kept under limit	Feed length ±0.1% of full length
	Heading	No waste is produced during heading. No deformation/bubbles/voids in bolt	0 waste produced 0 deformation in bolt.
	Bolt Ejection	Frictional heating of the machine kept under limit; Bolt fully exits machine	Heating = T_deform * (1/F. S)
MEASURE	Speed	Machine is running at the correct speed, and smoothly	Observe that machine runs uninterruptedly and is not noisy
	Slicing	The slicer properly acts as a door, and is cleanly cutting the material	Check sharpness of blade

Results

Machine Analysis with Calculations and Simulation

Hand calculations were used to approximate deflection and stresses in the frame. They can be found in Appendix B. The bottom plate will deflect during heading since the linear actuator will push against the mount. A diagram showing the forces and the resulting moment is shown in Fig. 9.

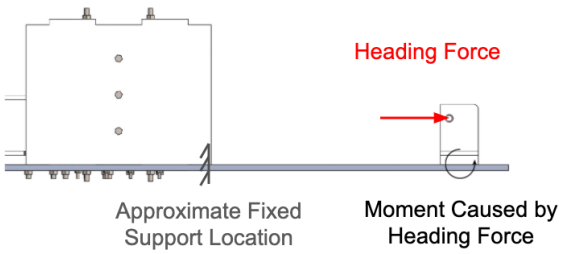

Fig. 9 – Forces and Moments on Bottom Plate

We know that the deflection in the bottom plate can be given by Eq. (1) [3]:

$$\delta_{max} = \frac{Ml^2}{2EI} \quad (1)$$

With the heading force, material properties and geometry, we calculated a rough deflection value of 0.6mm. This was then compared with a finite element model with exact geometry accounted for.

The simulation showed that there would be a maximum deflection of 1.3mm. This is relatively close to our rough deflection value from hand calculations. With this

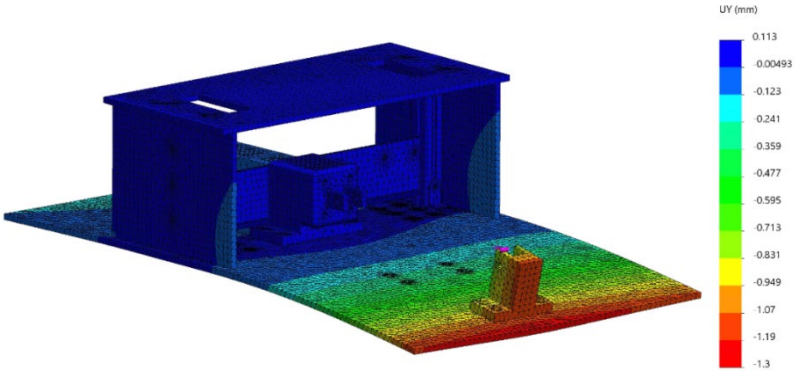

Fig. 10 – Full System Vertical Deflection Simulation undergoing Heading Operations

deflection value, we proceed to analyze the stresses in the dies and alignment rods during heading operation. With the 1.3mm of deflection, the linear actuator will push the dies together in the normal direction as intended, as well as in the vertical shear direction. Applying trigonometry and similar triangles, we found the vertical and horizontal components of the misalignment force.

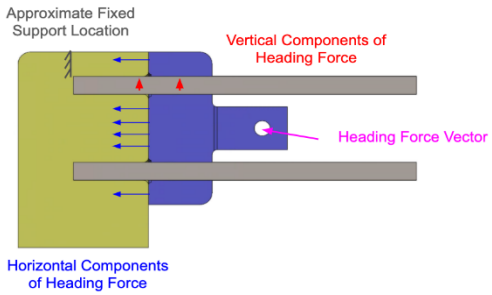

Fig. 11 – Vertical Components of Heading Force

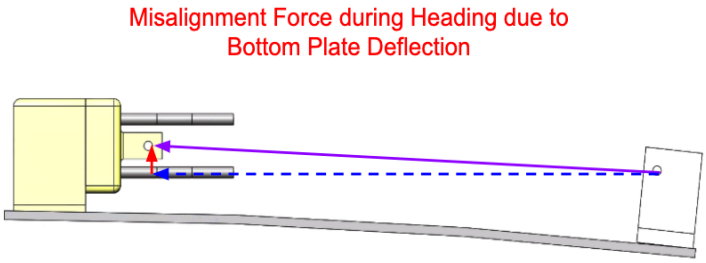

Fig. 12 – Misalignment Forces Due to Bottom Plate Deflection during Heading

From the FBD shown in Fig. 11 and Fig. 12, the upper die would react to the vertical misalignment force from the alignment rod. We know that the deflection and bending stress in a cantilevered beam are governed by Eq. (2) and Eq. (3) [3]:

$$\delta_{max} = \frac{PL^2}{3EI} \qquad \sigma_{bending,\,max} = \frac{PLy}{2I} \qquad (2)\ (3)$$

With the vertical heading force component, material properties, and geometry, we calculated a rough upper die maximum bending stress and strain of 7.92MPa and 0.34%, respectively. The hand calculations can be found in Appendix B. We then compared our calculations with simulation and had a maximum bending stress and strain value of 12.7 MPa and 0.45%. We are confident that the stresses will not cause yielding or cracking failure since the maximum stress does not exceed 14% of yield stress for the die material (ABS-M30). We also observed a maximum relative vertical displacement between the dies of 0.13mm. Our target tolerance for the alignment of the dies is ±0.25mm. Thus, we are confident that at maximum deformation of the frame and machine, the bolts will still be within tolerance specification.

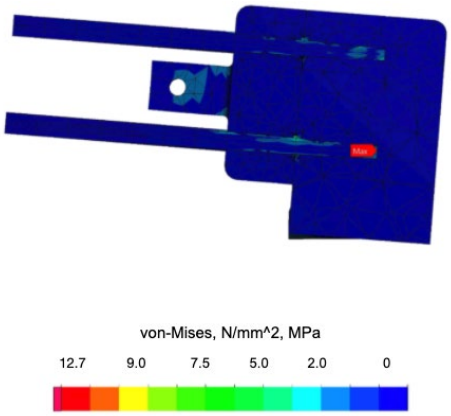

Fig. 13 – FEA Results for Dies – Von-Misses Stress

To validate our theoretical heading force, a simulation of the actual heading procedure can be used. Unfortunately, this simulation is very complex to set up and requires specialized metal forming software such as Deform or QForm. We have estimated the validity of our process using a forming limit diagram (FLD) [6].

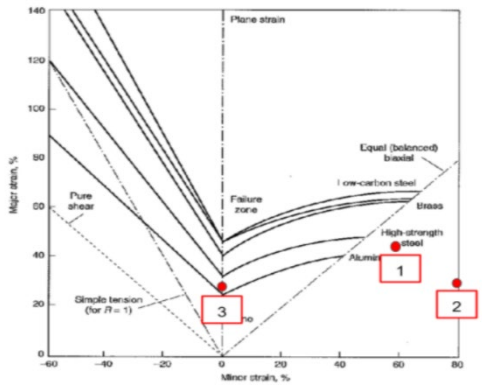

Fig. 14 – Forging Limit Diagram with Bolt Strains

Table 2 - Calculated Major/Minor Axis Strain

Path Line	Major Axis Strain (%)	Minor Axis Strain (%)
1	42.2%	60%
2	32.8%	80.0%
3	32.8%	0.0%

However, there are limitations with this methodology. FLD diagrams are made for sheet metal operations so the material limitations for sheet metal may not be the same as the limitations for a heading procedure.

Additionally, we can expect the FLD curves to change with temperature so the curves to the left may not accurately represent the forming limits for steel at elevated temperatures.

Downscaling

In real life, the Sutherland machine uses a crankshaft driven press powered by a 40hp motor providing up to 315 metric tons of force and a stroke length of 250mm. The Sutherland press also features a maximum die height of 500mm and maximum die base of 1120x840mm, allowing for a variety of different die geometries. The machine is controlled by an encoder that provides the operator with the punch's velocity and position and allows for CNC operations [2]. For our machine, we scaled down these parameters by switching to a 0.025 metric ton Progressive Actuator PA-14 mini linear actuator with a stroke length of 75mm [4]. The prototype machine has a maximum die height of 78mm and maximum die base of 72x64mm. The prototype machine heading force is also controlled using PA-14 current and load, with the current-load graph from the datasheet [4]. The prototype machine will use current to determine what load is applied and when to release the dies and eject the bolt.

Choice of Materials

Several methodologies have been used to choose materials in our design. For the base plate of the assembly, we have used FEA to validate our choice of A36 Steel. The sidewalls of our design are acrylic plates because of its low cost, ease of manufacturing, and because the walls are not subject to any major stress.

For our die and billet chamber, we use three Ashby charts [7] to determine the material best fit for the design, based on a list of set criterion. We start out with three materials that might be viable as shown in Table 3. Material data for the different materials was gathered from different sources [8] [9].

Table 3 – Material Properties used for Selection and Elimination

Material	Wear constant (1/MPa)	Hardness	Young's Modulus (GPa)	Strength (MPa)	Fracture Toughness ($MPa*m^{1/2}$)
H13 Tool Steel [8]	$3.0 * 10^{-6}$	45-50 HRC	210 – 215	1000 – 1380	130
ABS-M30 [9]	$2.1*10^{-8}$	60 – 70 Rockwell M	2.2 – 2.3	31 – 33	1.5
Polycarbonate [9]	$2.0*10^{-9}$	70 – 90 Rockwell M	2.2 – 2.5	61 – 69	4.1

1. Wear vs Hardness. We need to make sure that the die and chamber does not undergo significant wear during operation. Also, the chamber and die must be hard enough to withstand multiple heading operations.
2. Young's Modulus vs Strength. Yield and deformation are two of our primary concerns to avoid in the die and chamber. With either yield or deformation, continued operation of our machine might not be possible. It could at least produce bolts not up to specifications, and at worst, not be able to operate at all.
3. Fracture Toughness vs Strength. To be able to operate, our prototype must be able to resist fracturing. For this reason, fracture toughness and strength are key factors to avoid failure.

Based on Ashby charts shown in Appendix A, we can see that all the preselected materials are viable. By using either ABS-M30 or Polycarbonate, we can reduce cost significantly, because we can 3D print our prototype instead of machining and heat-treating H13 steel. We have decided to use ABS-M30, because of its sufficient material qualities and its superior friction constant to that of polycarbonate. Also, ABS-M30 is easily available at Jacobs for printing on the Stratasys printers, making it an accessible and affordable choice for our prototype.

Process Selection

For our prototype, we will be manufacturing most parts using either a laser cutter, CNC machine or 3D printing (using a Stratasys printer). Stratasys printers allow for accurate prints that will have a high enough resolution to properly test our prototype. We are using the laser cutter to create our acrylic sidewall and top plate, the

Stratasys 3D printer to create the heading chamber and die, and CNC for our bottom plate of steel. By using a silicone-based lubricant, we can achieve a better friction constant for our billet chamber and die. Use of lubrication also ensures that nothing sticks to the blade and machinery during the heading process.

Joints

We are using several joining methods for our build. For the acrylic plates that surround our build, we will be using a box joint to achieve a wall that is perpendicular to the floor of our design. This is a well-tested woodworking joint that is also applicable for acrylic plates. For the billet compartment, we are using a dowel joint to join the middle, front and end sections of the compartment. A dowel joint is also primarily a woodworking joint, that works well for 3D printed parts. This ensures our actuators will be properly secured in the billet compartment. For securing most parts to the bottom plate, we are using bolts, washers, and nuts. We are using L Brackets to attach the 25-25 Aluminum Extrusion to the frame. The metal inserts in the upper die will be inserted using a press fit and the rods that act as rails will be hot pressed into the lower die. We will also use a zip tie to further restrain the linear actuator to the middle holder and clevis pins to attach the linear actuator to the upper die and end mount.

Economic Considerations for Selection:

All design choices in the prototype have been done by selecting the lowest cost material that meets our machine specifications, and the process or tolerance that accurately represents a full-scale machine. For example, almost the entire design is 3D printed in ABS-M30 in a Stratasys printer. Minimal metal has been used in the design to keep the cost low. Necessary forces have been calculated, and actuators with an appropriate factor of safety have been chosen. Whenever metal has been chosen, careful material selection has been used to ensure the cost will stay low. Computer Numerical Controlled (CNC) machining is minimized only to parts that are necessary, such as the 4130-steel blade, which must be hardened and wear-resistant.

Conclusion:

1. Even with smaller heading forces from scaling down, high modulus materials such as A36 steel for machine components are still required in order to minimize misalignment between the dies.
2. Alignment features between the dies are critical to minimizing misalignment. If there is a lot of play between parts in the machine, then the amount of misalignment increases. Alignment rods are helpful because they can be tightly controlled for tolerancing and can also be very stiff.
3. It is essential to make design decisions to minimize deflection without over-constraining mechanisms for proper machine function and reliability.

Acknowledgements:

We would like to thank Professor Adi Ben-Artzy from UC Berkeley's Nuclear Engineering Department, Josh DeWitt from UC Berkeley's Mechanical Engineering department, and Chris Parsell from Jacobs Design Institute. Their extensive knowledge has been invaluable in our design process.

Bibliography:

1. *Heading Hints: A Guide to Cold Forming Specialty Alloys*. Carpenter Technology Corporation, 2001.
2. "HCP SERIES." *Sutherland Presses*, www.sutherlandpresses.com/trim-presses/hcp-series.
3. Budynas, Richard G. *Roark's Formulas for Stress and Strain*. New York: McGraw-Hill, 2002.
4. Progressive Automations. *PA-14 Data Sheet*. Progressive Automations.
5. Lin, Angie. *Fishbone (Ishikawa) Diagram Template for Root Cause Analysis*. 8 Oct. 2018, tulip.co/blog/leanmanufacturing/fishbone-ishikawa-diagram-for-root-cause-analysis/.
6. Woelke, Pawel B., Michael D. Shields, Najib N. Abboud, and John W. Hutchinson. "Simulations of Ductile Fracture in an Idealized Ship Grounding Scenario Using Phenomenological Damage and Cohesive Zone Models." Computational Materials Science. Elsevier, May 11, 2013.
7. Ashby, Michael F. *Materials Selection in Mechanical Design*. 2nd ed. Pergamon Press LTD, 1999.

8. “H13 Tool Steel Technical Data.” *Hudson Tool Steel Corporation*, Hudson Tool Steel Corporation, www.hudsontoolsteel.com/technical-data/steelH3.
9. FDM Material Choices and their mechanical properties. https://www.researchgate.net/figure/FDM-material-choices-and-their-mechanical-properties-Table-from_tbl1_311560257

Appendix A, Ashby Charts – Material Choice for Prototype

1. Wear vs. Hardness

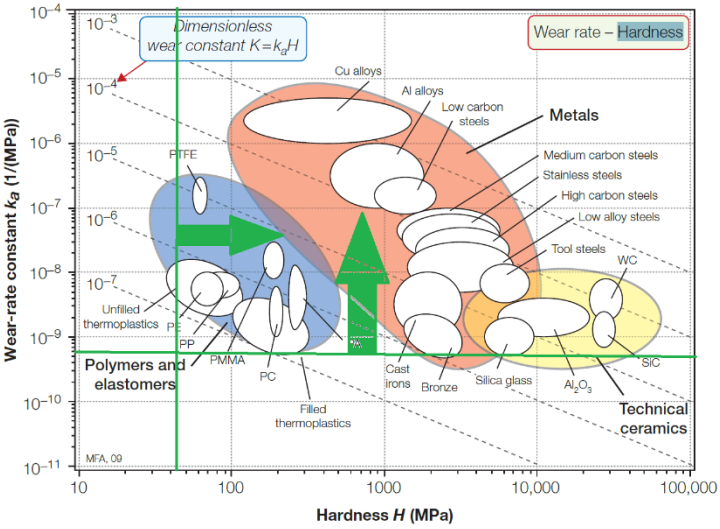

2. Young's Modulus vs. Strength

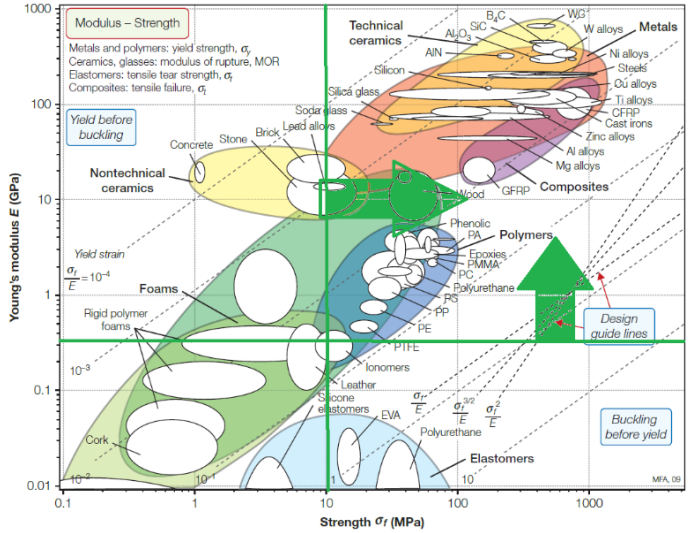

3. Fracture Toughness vs. Strength

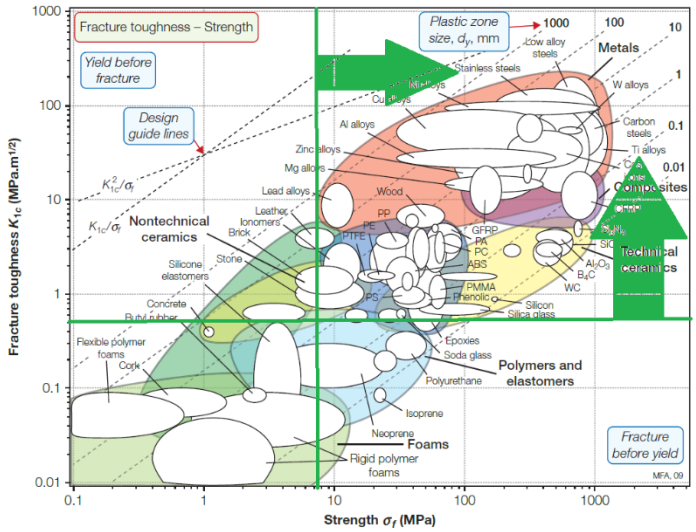

Appendix B, Hand Calculations

1. Heading Force Calculation

Heading Force (F) = (K)(Y)(A)

→ Impression Die Forging Constant (K) = 4

→ Flow Stress (Y) = $(k)(\varepsilon)^n$ = $(0.143)(0.2)^{0.167}$ = 0.1102 MPa

→ Assuming white plasticine

→ k = 0.143

→ ε = 0.2

→ n = 0.167

→ Area (A) from Solidworks

→ M10 = 339.61 mm^2

→ M20 = 679.22 mm^2

→ Heading Force (M10) = (4)(0.1102)(339.61) = **149.7N = 33.65 lbs**

→ Heading Force (M20) = (4)(0.1102)(679.22) = **299.4N = 67.31 lbs**

2. Bottom Plate Deflection Calculation

Bottom Plate Deflection

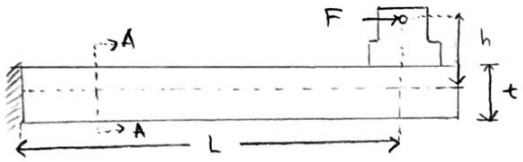

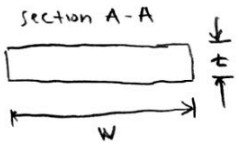

F - heading force
h - distance between linear actuator mount hole and plate N.A.
t - plate thickness
L - distance from "fixed" support to linear actuator mount hole center
w - plate width
δ - plate vertical deflection
E - elastic modulus of A36 steel
I - area moment of inertia

Equivalent Beam Problem:

$$\delta = \frac{ML^2}{2EI} = \frac{(Fh)L^2}{2E\left(\frac{1}{12}wt^3\right)} = \frac{(310N)(49mm)(320mm)^2}{2\left(190000\frac{N}{mm^2}\right)\frac{1}{12}(400mm)(6mm)^3}$$

$\delta = 0.6mm$

3. Die Misalignment Calculation

Die Misalignment

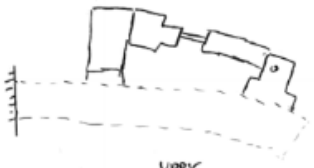

Force Vector, using trigonometry

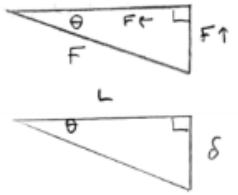

$\tan^{-1}\left(\frac{\delta}{L}\right) = \tan^{-1}\left(\frac{1.3mm}{320mm}\right) = 0.23°$

$F = 310N$

$F\uparrow = F\sin\theta \approx 2\ N$

$F\leftarrow = F\cos\theta = 309.9N \approx 310N$

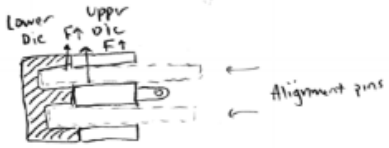

$F_\uparrow$ - upwards force component of heading force

L - lower die alignment pin contact length

t - beam thickness

E - elastic modulus of ABS M30 in ZX orientation (weakest orientation)

I - area moment of inertia

D - alignment pin diameter

δ - lower die vertical deflection

Equivalent beam problem

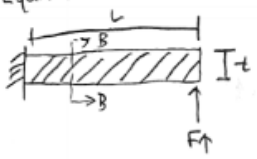

Section B - B

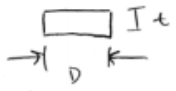

$\delta_{max} = \frac{FL^3}{3EI} = \frac{(F_\uparrow)(L^3)}{3E\left(\frac{1}{12}\right)(D)(t)^3} = \frac{(2N)(28mm)^3}{3\left(2300\frac{N}{mm^2}\right)\frac{1}{12}(8mm)(10mm)^3}$

$\delta_{max} = 0.02\ mm$

Maximum gap between alignment pin and upper die rail insert

Alignment pin diameter tolerance: $8mm \pm 0.05mm$

Insert ID tolerance: $8.1\ mm \pm 0.025mm$

Largest gap when Alignment pin $\phi = 7.85mm$, Insert ID $= 8.125mm$ — Max gap $= 0.15mm$

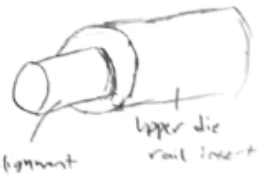

Max gap + Max deflection $\approx 0.20\ mm$